


RESEARCH ARTICLE

Clusterin contributes to early stage of Alzheimer's disease pathogenesis

Shin-Bi Oh¹, Min Sun Kim¹, SuJi Park¹, HyunJu Son¹, Seog-Young Kim^{1,2}, Min-Seon Kim³, Dong-Gyu Jo⁴, Eunyoung Tak^{1,2}, Joo-Yong Lee^{1,2} 

¹ Asan Institute for Life Sciences, Asan Medical Center, Seoul, Republic of Korea.

² Department of Convergence Medicine, University of Ulsan College of Medicine, Seoul, Republic of Korea.

³ Department of Endocrinology and Metabolism, University of Ulsan College of Medicine, Seoul, Republic of Korea.

⁴ The School of Pharmacy, Sungkyunkwan University, Suwon, Republic of Korea.

Keywords

Alzheimer's disease, amyloid pathology, apolipoprotein J, A β oligomers, chaperone protein

Corresponding author:

Joo-Yong Lee, PhD, Asan Institute for Life Sciences, Asan Medical Center, 388-1 Poongnapdong, Songpagu, Seoul 05505, Republic of Korea, Phone and Fax: +82-2-3010-4143 (E-mail: jlee@amc.seoul.kr)

Received 26 June 2018

Accepted 28 September 2018

Published Online Article Accepted

8 October 2018

doi:10.1111/bpa.12660

Abstract

While clusterin is reportedly involved in Alzheimer's disease (AD) pathogenesis, how clusterin interacts with amyloid- β (A β) to cause A β neurotoxicity remains unclear *in vivo*. Using 5 \times FAD transgenic mice, which develop robust AD pathology and memory deficits when very young, we detected interactions between clusterin and A β in the mouse brains. The two proteins were concurrently upregulated and bound or colocalized with each other in the same complexes or in amyloid plaques. Neuropathology and cognitive performance were assessed in the progeny of clusterin-null mice crossed with 5 \times FAD mice, yielding *clu*^{-/-};5 \times FAD and *clu*^{+/+};5 \times FAD. We found far less of the various pools of A β proteins, most strikingly soluble A β oligomers and amyloid plaques in *clu*^{-/-};5 \times FAD mice at 5 months of age. At that age, those mice also had higher levels of neuronal and synaptic proteins and better motor coordination, spatial learning and memory than age-matched *clu*^{+/+};5 \times FAD mice. However, at 10 months of age, these differences disappeared, with A β and plaque deposition, neuronal and synaptic proteins and impairment of behavioral and cognitive performance similar in both groups. These findings demonstrate that clusterin is necessarily involved in early stages of AD pathogenesis by enhancing toxic A β pools to cause A β -directed neurodegeneration and behavioral and cognitive impairments, but not in late stage.

INTRODUCTION

Alzheimer's disease (AD) is a progressive neurodegenerative disease and the most common type of dementia in the elderly. Early investigation of the cause of AD supported the amyloid hypothesis of pathogenesis in which accumulation of amyloid- β (A β), derived from proteolytic cleavage of amyloid precursor protein (APP), leads to neurodegeneration. Recent efforts have aimed to find risk factors other than A β that may contribute to late-onset AD, which is the phenotype in most cases of the disease.

Clusterin, also known as apolipoprotein J (Apo J), has been identified as an important risk factor for late-onset AD by large-scale GWAS (17,24). Clusterin is a ubiquitously expressed glycoprotein and is present in very high levels in the brain. In patients with AD, clusterin levels are even higher in the brain (14,33,40), serum and cerebrospinal fluid (CSF) (8,13). Clusterin is found to colocalize with A β in the amyloid deposits of brains of AD patients (8,22,34).

Clusterin, the first reported extracellular mammalian chaperone protein (20,42), binds to biologically active hydrophobic residues exposed on misfolded or aggregated A β proteins (43,44), including toxic oligomers, to prevent further aggregation, render them susceptible to degradation, or suppress their toxicity. Accordingly, clusterin was shown to decrease A β -induced neurotoxicity in rodent hippocampal neurons (4) and attenuate the toxic effects of A β oligomers in a novel *in vivo* model of *Caenorhabditis elegans* (2). Other studies have demonstrated that A β -bound clusterin facilitates the clearance of A β across the blood-brain barrier (BBB) (3,57). A β oligomers pre-incubated with clusterin induced less neuronal death and learning and memory impairment in rats compared with A β oligomers without clusterin (7). These findings support protective mechanisms by which clusterin may inhibit AD pathogenesis.

However, increasing evidence suggests that clusterin also specifically interacts with A β oligomers to exacerbate their toxicity. When clusterin binds to toxic A β oligomers, it sequesters and stabilizes the oligomeric structures,

interfering with their further aggregation into less toxic fibril aggregates (41). Clusterin binding has been shown to shield A β oligomers from enzymatic degradation (32,37,38). Clusterin augmented A β toxicity in PC12 cells or organotypic mouse brain slice cultures in parallel with the formation of clusterin-induced and -stabilized A β oligomers (25,40,41). Knockdown of clusterin in primary neurons reduced A β toxicity (23), and the genetic ablation of clusterin (*clu*^{-/-}) in PDAPP mice that develop AD pathology caused significantly fewer amyloid deposits and less neuritic dystrophy with no alteration of the total A β deposition (10). More interestingly, a clinical longitudinal study (11) found significant associations between levels of clusterin and A β in CSF and entorhinal cortex atrophy seen on MRI, implying that clusterin-A β interaction is important in the earliest stages of AD pathogenesis.

In the present study, we evaluated the effect of genetic deletion of clusterin on amyloid pathogenesis and motor and cognitive behavioral performance in 5 \times FAD transgenic mice, which co-express five familial hAPP/PS1 mutations and develop severe AD pathology at an early age (39). The results provide the first *in vivo* evidence that clusterin is an important endogenous factor facilitating the early stage of AD pathogenesis, but its influence is attenuated or lost in the late stage when amyloid deposition is already quite advanced.

MATERIALS AND METHODS

Animal studies

This animal study was approved by the Institutional Animal Care and Use Committee of the Asan Institute for Life Sciences, Asan Medical Center (Seoul, Korea).

Clusterin-deficient (*clu*^{-/-};5 \times FAD) and their littermate 5 \times FAD mice (*clu*^{+/+};5 \times FAD) were obtained by breeding clusterin-null mice (*clu*^{-/-}) (10,35) with 5 \times FAD transgenic mice, which co-express hAPP₆₉₅ with three familial AD mutations (K670N/M671L, I716V and V717I) and presenilin (PS1) with two familial mutations (M146L and L286V) (39). Experiments were performed with 5- and 10-month-old male and female mice. All animals were bred and housed with free access to food and water at 22.0°C \pm 1°C and with a 12-h light–dark cycle.

Tissue preparation and histologic or immunohistochemical examination

Shortly after completing the behavioral tests described below, the animals were killed under deep anesthesia. The cerebral hemispheres were divided, snap-frozen in liquid nitrogen and immediately stored at -80°C. Sagittal 12- μ m thick sections of the left hemisphere were serially mounted on 1% poly-L-lysine-coated glass slides using a cryostat (HM550; Microm, Walldorf, Germany).

Brain A β deposition was evaluated by immunohistochemistry using an anti-A β (17–24) antibody (4G8; BioLegend, San Diego, CA, USA). The sagittal sections

were fixed with 4% paraformaldehyde and briefly incubated in 70% formic acid (FA). Endogenous peroxidase activity in the tissue was depleted by treatment with 3% hydrogen peroxide, and the sections were blocked with 3% normal serum and 0.3% Triton X-100 in phosphate buffered saline (PBS) and reacted with the primary antibody (4G8; dilution, 1:200) and then with a biotinylated secondary antibody (Vector Laboratories, Burlingame, CA, USA). Finally, the sections were treated with avidin horseradish peroxidase (Vector Laboratories) and developed with 0.015% 3,3'-diaminobenzidine (DAB) and 0.001% hydrogen peroxide (Vector Laboratories). For immunofluorescent examination, the 4G8-immunoreacted tissues were visualized with Alexa Fluor-conjugated secondary antibodies (Thermo Fisher Scientific, Waltham, MA, USA).

To detect colocalization of clusterin and A β in amyloid deposits, the brain tissues were immunologically co-stained with the primary antibodies, anti-A β (4G8) and anti-clusterin/Apo J (Novus Biologicals, Littleton, CO, USA; dilution, 1:100) antibodies and then with two corresponding fluorescent secondary antibodies, Alexa Fluor 488- and 555-conjugated antibodies.

To examine congophilic compact amyloid plaques, brain sections were stained with Hematoxylin QS (a modification of Mayer's hematoxylin; Vector Laboratories) and Accustain[®] Congo red amyloid staining solution (Sigma-Aldrich, St. Louis, MO, USA) (26). After washing with absolute ethanol, the stained tissue sections were examined for congophilic plaques using a light or polarized microscope (Eclipse 800i; Nikon, Tokyo, Japan). For further analysis, microscopic images of stained tissues were captured with a DS-Fil digital camera connected to NIS-Elements image processing software (Nikon).

Because compact amyloid plaques emit blue fluorescence *in situ* under UV illumination (26), we examined blue fluorescent amyloid deposits in the brain tissues under a fluorescence microscope (Eclipse 800i) with a UV-2A filter (dichroic, 400 nm; excitation, 330–380 nm; barrier, 420 nm).

The load of amyloid deposits or plaques in the brain was expressed as the per cent area of 4G8-immunoreactive deposits or the number of congophilic plaques per mm² in regions of interest from the hippocampal, cortical and thalamic areas.

Quantitative real-time polymerase chain reaction (PCR) assay

Total RNAs were extracted from the right hemispheres using the RNeasy Mini Kit (QIAGEN, Valencia, CA, USA) and cDNAs were generated using the iScript[™] cDNA synthesis kit (Bio-Rad, Hercules, CA, USA). The quantitative RT-PCR was conducted with the Bio-Rad CFX connect Real-time PCR machine using sense and antisense primers (250 nM each; Macrogen, Seoul, Korea) with 5 \times HOT FIREPol[®] EvaGreen[®] qPCR Supermix (Solis BioDyne, Tartu, Estonia). The sequences of sense and anti-sense primers used were as follows: for clusterin (Apo J;

NM_013492), 5'-CAG TTC CCA GAC GTG GAT TT-3' and 5'-TCC TGG CAC TTT TCA CAC TG-3', for Apo E (BC083351), 5'-TGT CCT GCA ACA ACA TCC AT-3' and 5'-TAT TAA GCA AGG GCC ACC AG-3', for Dickkopf Wnt signaling pathway inhibitor 1 (DKK-1; NM_010051), 5'-CCT TCG GAG ATG ATG GTT GT-3' and 5'-GTT CTT GAT CGC GTT GGA AT-3' and for GAPDH (NM_008084), 5'-AGG TCG GTG TGA ACG GAT TTG-3' and 5'-TGT AGA CCA TGT AGT TGA GGT CA-3', respectively. Finally, mRNA expression levels were calculated relative to that of GAPDH using the $\Delta\Delta C_t$ method (27).

Quantitative enzyme-linked immunosorbent assay (ELISA)

After the right brain hemispheres were weighed, they were homogenized in PBS (pH 7.4; 1:10, w/v) containing protease inhibitors (cOmplete™ Protease Inhibitor Cocktail; 1 tablet/50 mL; Roche Diagnostics, Mannheim, Germany) and centrifuged at $100\,000 \times g$; the supernatant was then collected (the PBS-soluble fraction). The pellets were sonicated in 2% SDS in PBS, and the SDS-soluble fraction was collected by centrifugation at $100\,000 \times g$. Finally, the SDS-insoluble pellets were solubilized in 70% FA and the FA-soluble fraction was collected by centrifugation at $100\,000 \times g$.

We subjected the PBS-, SDS- and FA-soluble fractions to sandwich ELISA for quantification of human A β 40 and A β 42 (Thermo Fisher Scientific). Analysis of FA-soluble fractions was preceded by neutralization with 1 M Tris (adjusted to pH 11.0 using 5 M NaOH). In addition, the quantification of oligomeric A β s (oA β) in PBS- and SDS-soluble fractions and A β aggregates (aA β) in SDS extracts was performed using an Oligomeric A β ELISA kit (BioSensis, Thebarton, SA, Australia) and an A β aggregate ELISA kit (Thermo Fisher Scientific), respectively.

We also measured the amount of clusterin in the brain tissue (SDS extracts) using a SimpleStep® ELISA kit for mouse clusterin (Abcam, Cambridge, UK).

All measurements were taken at 450 nm using the Synergy H1 Hybrid microplate reader (BioTek, Winooski, VT, USA).

Immunoblotting and co-immunoprecipitation analysis

The following primary antibodies were used for immunoblotting: anti-A β (1–16) (6E10; BioLegend; dilution, 1:2000), anti-clusterin/Apo J (Novus Biologicals; 1:1000), anti-apolipoprotein E (Apo E; Santa Cruz Biotechnology, Santa Cruz, CA, USA; 1:1000), anti-DKK-1 (Dickkopf-1; Boster, Pleasanton, CA, USA; 1:1000), anti-NeuN (Merck Millipore, Darmstadt, Germany; 1:500), anti-nonphosphorylated neurofilament protein SMI-32 (BioLegend; 1:2000), anti-synaptophysin (Santa Cruz Biotechnology; 1:5000), anti-ankyrin G (Santa Cruz Biotechnology; 1:2000), anti-PSD95 (postsynaptic density protein 95; Applied Biological Materials, Richmond, Canada; 1:2000), anti-VAMP

(vesicle-associated membrane protein)/synaptobrevin (Santa Cruz Biotechnology; 1:1000), anti-ProSAP2 (postsynaptic scaffold protein)/Shank 3 (Santa Cruz Biotechnology; 1:500) and anti- β -actin (Sigma-Aldrich; 1:2000) antibodies.

Brain hemispheres were homogenized in PBS (pH 7.4; 1:10, w/v) containing protease inhibitors (cOmplete™ Protease Inhibitor Cocktail), and the lysates were collected by centrifugation at $15\,000 \times g$. The amount of protein in the lysate was measured using a bicinchoninic acid assay (Bio-Rad).

For Western blot analysis, proteins were prepared in sample buffer [62.5 mM Tris (pH 6.8), 2% SDS, 10% glycerol, 0.01% bromophenol blue, 5% mercaptoethanol and 50 mM dithiothreitol], and then separated by SDS-polyacrylamide gel electrophoresis and transferred onto polyvinylidene difluoride (PVDF) membranes (Merck Millipore) using semidry blotters (TE70 PWR; Amersham Biosciences, Uppsala, Sweden). To detect A β proteins, protein lysates in tricine sample buffer [200 mM Tris-HCl (pH 6.8), 40% glycerol, 2% SDS and 0.04% Coomassie Blue G-250; Bio-Rad] were electrophoresed on 10%–20% Mini-PROTEAN™ Tris-Tricine Precast Gel (Bio-Rad) under nonreducing conditions. After blocking with 5% skim milk and 1% BSA in TBS-T buffer (25 mM Tris, 150 mM NaCl, 0.1% Tween 20; pH 7.4), the blot was reacted with a primary antibody and subsequently with a horseradish peroxidase-conjugated secondary antibody (Santa Cruz Biotechnology).

To determine interactive complexes of A β peptides and clusterin in the brain, we immunoprecipitated brain lysates (containing 800 μ g of total protein) with anti-A β (1–16) antibody (6E10) plus Protein G-sepharose beads (GE Healthcare, Buckinghamshire, UK) or anti-clusterin/Apo J antibody (Novus Biologicals) plus Protein G-sepharose beads. After washing in PBS, the protein/antibody-bound beads were eluted in tricine sample buffer [200 mM Tris-HCl (pH 6.8), 40% glycerol, 2% SDS and 0.04% Coomassie Blue G-250]. Shortly thereafter, the supernatant protein samples were collected by brief centrifugation and fractionated by electrophoresis on 10%–20% Tris-Tricine Precast Gel (Bio-Rad) under nonreducing conditions. Finally, the proteins were detected by Western blot using anti-A β antibody (6E10) or anti-clusterin/Apo J antibody.

Immunoreactive proteins were visualized using ECL™ Prime Western Blotting Detection Reagent (GE Healthcare) with the Davinch-Western™ Chemiluminescence Imaging System (CAS-400SM; Davinch-K, Seoul, Korea). The band intensities were measured using ImageJ software (National Institutes of Health, Bethesda, MD, USA), and protein levels were normalized to those of β -actin.

Cognitive and motor behavioral analysis

Five- or 10-month-old mice were tested for spatial learning and memory in a Morris water maze (MWM) consisting of a circular plastic pool (120-cm in diameter) with a cylindrical escape platform (10-cm in diameter) in the northwest quadrant of the pool, 0.5-cm under the surface

of opaque water (maintained at $21.0^{\circ}\text{C} \pm 1.0^{\circ}\text{C}$) and with three visual cues on the wall. For 5 consecutive days, the animals were given daily training to swim and find the hidden escape platform. Each day, they had three 60-s trials, each starting at a different quadrant (northeast, southeast and southwest quadrant). Three hours after the final training, the mice performed a probe trial for 60-s starting from the southeast quadrant with the escape platform removed. The time, path and distance spent

swimming in the pool as well as the frequency the target zone was crossed trying to locate the platform were monitored with SMART Video Tracking System (Harvard Apparatus, Holliston, MA, USA).

For the following 3 days, the same mice were given a balance beam task to evaluate balance and motor coordination. The beam was a flat wooden bar (1.2-cm wide, 80-cm long) connected to two 40-cm high support columns. A dark escape chamber was located at the opposite end

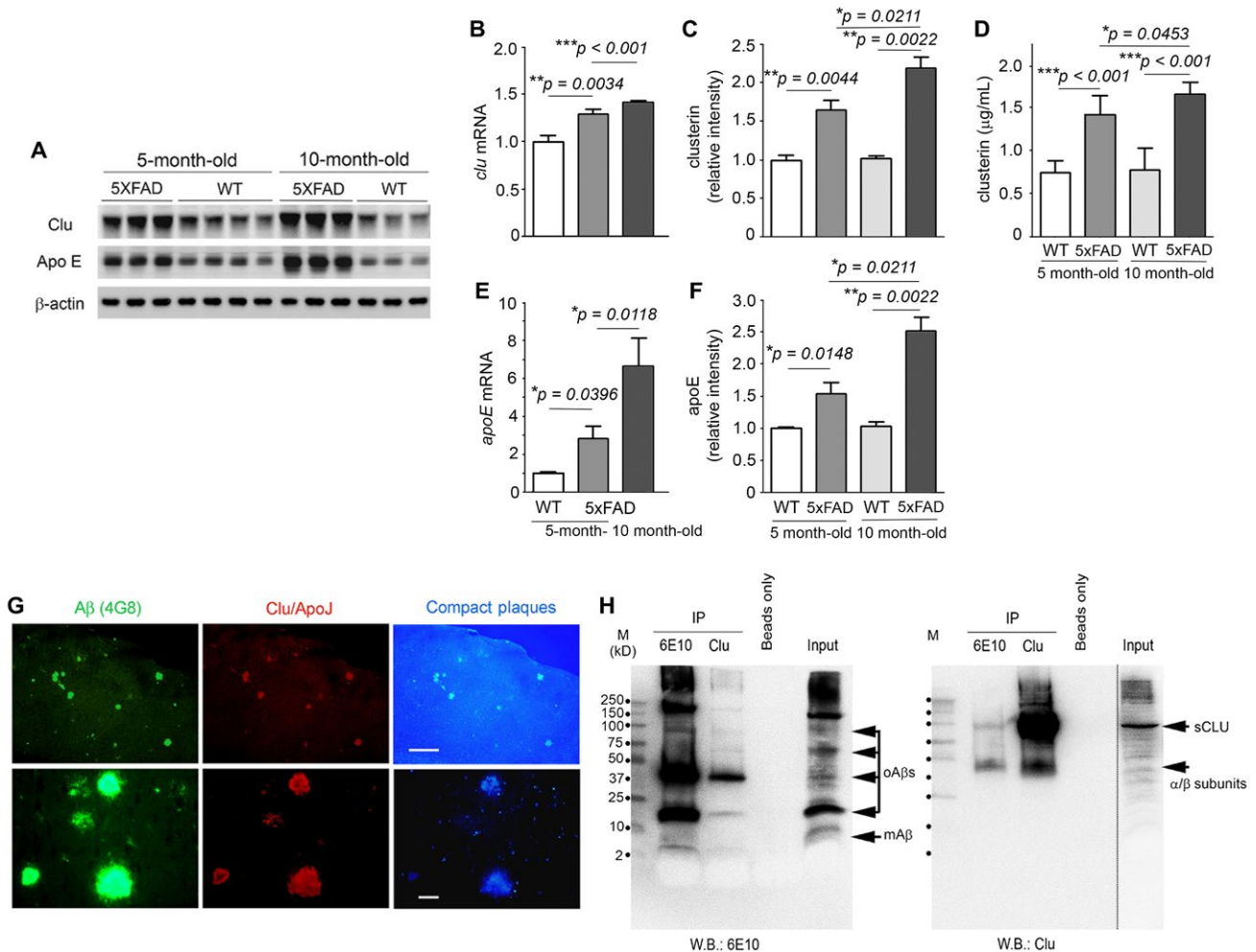


Figure 1. Interactions between clusterin and A β in the brains of 5x FAD mice. **A.** Representative Western blots show expression or deposition of clusterin (Clu), Apo E and β -actin (as a loading control) in the brains of 5- or 10-month-old 5x FAD mice and their wild-type littermates (WT). **B** and **E.** Clusterin (**B**) or Apo E (**E**) mRNA levels were measured by quantitative real time PCR. Values were calculated relative to that of GAPDH and bars are presented as fold changes relative to control values (5-month-old wild-type mice) ($n = 6-10$ for all groups). **C** and **F.** Graphs show densitometric quantification of clusterin (**C**) or Apo E (**F**) from representative blots (**A**). After normalization with β -actin, the fold of change is presented as compared to control (5 month-old wildtype mice) ($n = 3-4$ for all groups). **D.** ELISA quantification of mouse clusterin from SDS extracts ($n = 6-9$ for all groups). Data represent mean \pm SEM of three independent experiments. * $P < 0.05$, ** $P < 0.01$, or *** $P < 0.001$. **G.** Fluorescence microphotographs show

colocalization of A β (green) and clusterin (red) in compact amyloid plaques (blue). After double immunofluorescence staining with anti-A β (17-24) (4G8) and anti-clusterin (Clu)/Apo J antibodies, the brain tissues were examined at lower ($\times 40$, top row) and higher ($\times 400$, bottom row) magnifications under the appropriate fluorescence filters. Scale bars, 500 μm (top row) and 50 μm (bottom row). **H.** Brain lysates (800 μg) were immunoprecipitated (IP) using either anti-A β (1-16) (6E10) or anti-clusterin (Clu) antibody, and the precipitates were subjected to Western blot (W.B.) with anti-A β (1-16) (6E10) (left panel) or anti-clusterin antibody (Clu; right panel). Beads only and input samples (50 μg as total protein) show negative and positive signals, respectively. The numbers along the 1st lane (M, molecular marker) of each blot denote the molecular sizes (kD). mA β , A β monomers; oA β s, A β oligomers; sCLU, secretory clusterin; α/β subunits, α or β subunits of clusterin.

from where the mice were placed on the beam. The test was conducted in dim light with brighter illumination condensed on the starting point of the beam. The mice were encouraged to move from the starting point to the escape chamber on the other end. They were trained with three 90-s trials per day with a 15-min interval between trials. The time it took for the mice to traverse the beam and enter the chamber was recorded. If a mouse fell off the beam, we excluded that trial and conducted another trial. If a mouse stayed on the beam but did not reach the chamber within 90-s, the maximum time was recorded as 90-s.

Statistics

Data are presented as the means \pm standard errors of the mean. Statistical comparisons between the groups were performed with an unpaired *t*-test or one-way ANOVA with Student–Newman–Keuls post hoc test, using Prism (GraphPad Software, La Jolla, CA, USA). Differences were considered significant at $P < 0.05$.

RESULTS

Interactive expression of A β and clusterin in the brains of 5 \times FAD mice

We evaluated the expression levels of clusterin in the brains of 5 \times FAD mice and their wild-type littermates. In qRT-PCR or Western blot analysis (Figure 1A–C), we found that 5 \times FAD mice expressed higher levels of clusterin than their littermates at the same age (5 or 10 months of age) and had a significant increase in clusterin levels from 5 to 10 months of age. In the wild-type littermates, there was no significant difference in clusterin levels between 5 and 10 months of age. The increases in clusterin levels in the 5 \times FAD mice were also detectable by quantitative ELISA measurement of mouse clusterin in the brain lysates (Figure 1D). In addition, there were similar patterns of elevation of apolipoprotein E (Apo E) (Figure 1A, E and F) and DKK-1 (Supplementary Figure S1) in 5 \times FAD mice. These findings indicate that A β deposition leads to the increased expression of clusterin, Apo E or DKK-1 in the brain.

5 \times FAD mice not only produce abundant levels of A β but also develop A β deposits or amyloid plaques in their brain at a relatively young age (39). A β -specific 4G8-immunohistochemistry detected a number of amyloid plaques throughout the brain tissues of 5-month-old 5 \times FAD mice, primarily identified as compact core amyloid plaques by their *in situ* emission of blue fluorescence under ultraviolet (UV) illumination (26) (Figure 1G). In line with studies of human brains affected with AD (6,8,22), we found close colocalization of clusterin and A β immunoreactivities in compact core amyloid plaques (Figure 1G).

To explore *in vivo* interactions between clusterin and A β , we performed co-IP experiments with brain lysates of 5 \times FAD mice (Figure 1H). When proteins

co-immunoprecipitated with anti-A β antibody (6E10) were fractionated under nonreducing conditions and then immunoblotted with anti-clusterin antibody, we found two sizes of clusterin, 40-kD α/β subunits and 80-kD mature secretory clusterin (sCLU). Additionally, reverse co-IP, which used anti-clusterin antibody and anti-A β antibody (6E10) for IP and Western blot, respectively, detected multiple forms of A β (monomers, dimers, oligomers and high-molecular-weight A β aggregates). These results thus suggest that clusterin and A β interact with each other *in vivo*, where clusterin interacts or binds with different A β structures.

Effects of genetic deletion of clusterin on amyloid pathogenesis

To investigate whether clusterin is implicated in amyloid pathogenesis, we compared the deposition of A β in the brains of *clu*^{+/+};5 \times FAD and *clu*^{-/-};5 \times FAD mice at 5 or 10 months of age. Western blot analysis revealed that A β was prominently upregulated with age in both *clu* genotypes of 5 \times FAD mice as their entire blot signals became more intense at 10 than at 5 months of age (Figure 2A). In contrast, the A β signals were generally attenuated in *clu*^{-/-};5 \times FAD mice compared with those in *clu*^{+/+};5 \times FAD mice at 5 months of age, whereas the *clu* genotype-related differences in A β intensities were undetectable at 10 months of age. Notably, significant differences among the groups were observed in band intensities of A β monomers, dimers and oligomers (with molecular sizes ranging from approximately 4.0 kD to 50.0 kD).

Next, to further elaborate the differences in A β deposition, we measured the amounts of various A β peptides in the brains of *clu*^{+/+};5 \times FAD and *clu*^{-/-};5 \times FAD mice. We used ELISA to quantify the levels of soluble A β 40 or A β 42 and A β oligomers in PBS- and SDS-soluble fractions and insoluble A β 40 or A β 42 in FA-soluble fractions in serially fractionated brain lysates. Total A β 40 or A β 42 amounts were calculated as the sum of the soluble and insoluble fractions of A β 40 or A β 42. A β aggregates were also analyzed in SDS extracts collected by brief centrifugation at 10 000 \times g but without ultracentrifugal fractionation. The levels of soluble, insoluble and total A β 40 or A β 42 were lower in 5-month-old *clu*^{-/-};5 \times FAD mice than in *clu*^{+/+};5 \times FAD mice (by 24.4%–63.8%; $P = 0.0064$ –0.0853) (Figure 2B and C), demonstrating that total A β (sum of A β 40 and A β 42) level was significantly lower in *clu*^{-/-};5 \times FAD mice (by 41.0%; $P = 0.0153$) (Figure 2D). Differences in A β 42 levels were even more striking, with soluble A β 42 levels in *clu*^{-/-};5 \times FAD mice 49.5% lower than those in *clu*^{+/+};5 \times FAD mice ($P = 0.0118$) and insoluble A β 42 35.7% lower ($P = 0.0309$) (Figure 2C). Soluble A β oligomers were also markedly lower in *clu*^{-/-};5 \times FAD mice (by 60.9%; $P < 0.0001$), but A β aggregates were only slightly lower (by 11.1%; $P = 0.2617$) (Figure 2D). From 5 months to 10 months of age, the levels of all pools of A β proteins (total, soluble and insoluble A β 40 or A β 42, A β oligomers and A β aggregates) were significantly or slightly increased

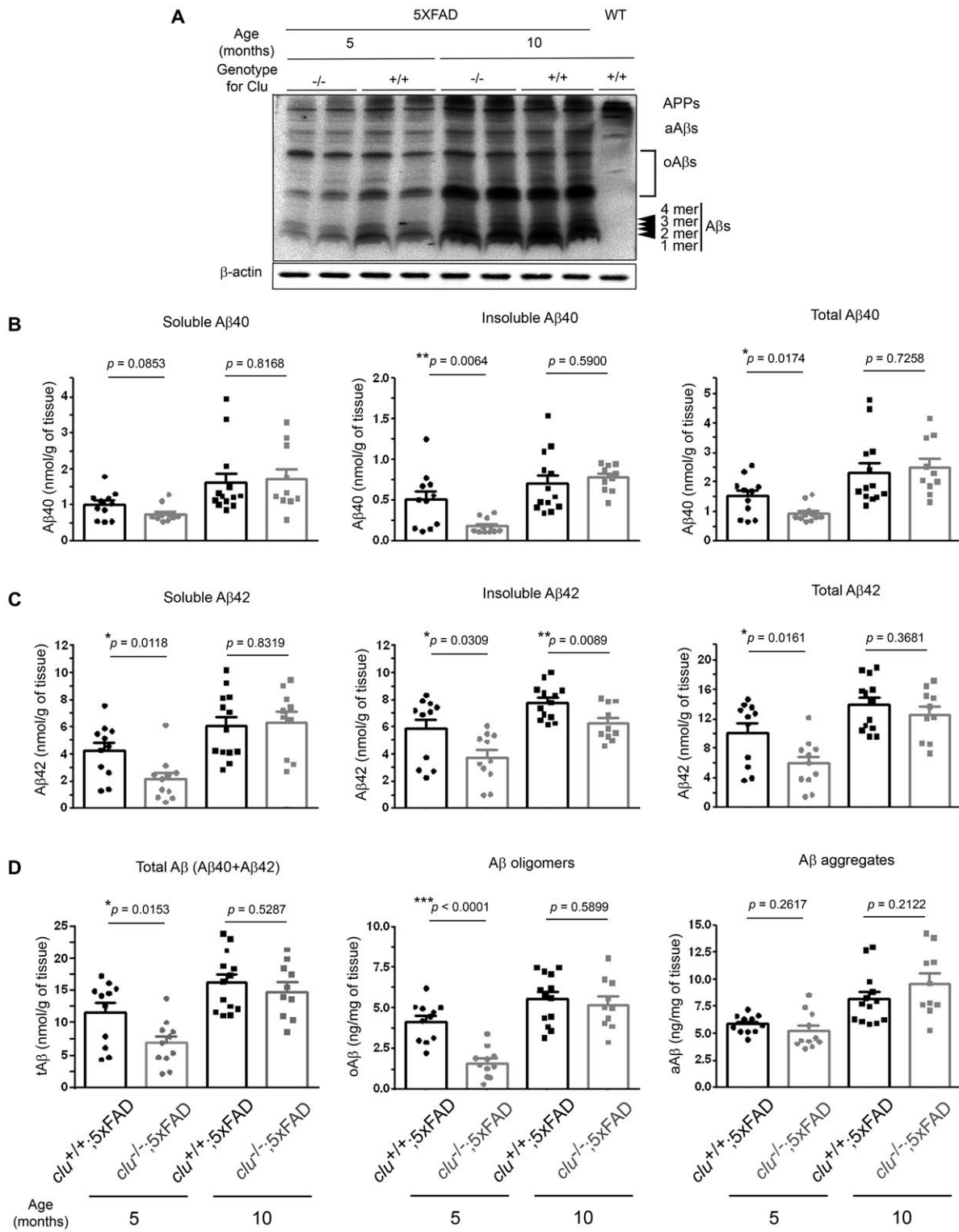


Figure 2. Deposition of various pools of brain A β in *clu*^{+/+};5 \times FAD and *clu*^{-/-};5 \times FAD mice. **A.** Representative Western blot shows expression or deposition of multiple sizes of A β proteins in the brains of *clu*^{+/+};5 \times FAD and *clu*^{-/-};5 \times FAD mice at 5 or 10 months of age. After immunoblotting with anti-A β (1–16) antibody (6E10) (top panel), the blot was deprobed and reacted again with anti- β -actin antibody as a loading control (bottom panel). Blot signals from a wild-type littermate mouse are shown on the right end of the blot (lane 9). oA β s, A β oligomers; aA β s, A β aggregates. **B–D.** ELISA quantification shows the deposition of various pools of A β proteins. Soluble (1st column) and insoluble (2nd column) A β 40 (**B**) or A β 42 (**C**) were analyzed from PBS- and SDS-soluble fractions, and FA-soluble fractions of brain lysates, respectively.

Total levels of A β 40 (**B**, 3rd column), A β 42 (**C**, 3rd column) and A β (**D**, 1st column) were calculated as the sum of soluble and insoluble A β 40, A β 42 and total A β 40 and total A β 42, respectively. Soluble A β oligomers (oA β) were quantified from PBS- and SDS-soluble fractions (**D**, 2nd column), whereas A β aggregates (aA β) were analyzed from SDS extracts without ultracentrifugal fractionation (**D**, 3rd column). All ELISA analyses were performed in duplicate. Numbers (males and females) of animals included in each group were 11 (5 and 6; for 5-month-old *clu*^{+/+};5 \times FAD), 11 (5 and 6; for 5-month-old *clu*^{-/-};5 \times FAD), 13 (6 and 7; for 10-month-old *clu*^{+/+};5 \times FAD) or 10 (5 and 5; for 10-month-old *clu*^{-/-};5 \times FAD mice). * P < 0.05, ** P < 0.01, or *** P < 0.001.

in both *clu* genotypes of 5 \times FAD mice (Figure 2B–D), resulting in no differences in the levels of all pools of A β proteins between *clu*^{-/-};5 \times FAD and *clu*^{+/+};5 \times FAD mice at 10 months of age (Figure 2B–D), except that insoluble A β 42 was 20.0% lower in *clu*^{-/-};5 \times FAD mice (P = 0.0089) (Figure 2C).

From these results for A β , we calculated the proportion of each pool or form of A β within the total amount of A β (sum of A β 40 and A β 42). First, we found neither *clu* genotype-related nor age-related differences in the ratio of total soluble or insoluble A β to total A β (Supplementary Figure S2A and S2B). However, compared with *clu*^{+/+};5 \times FAD mice, *clu*^{-/-};5 \times FAD mice at 5 months of age had a significantly lower ratio of soluble A β oligomers to total A β or to A β aggregates (by 34.6% or 52.9%; P = 0.0145 or 0.0002), whereas those ratios in both *clu* genotypes were not significantly different at 10 months of age (Supplementary Figure S2C and S2E). The proportion of A β oligomers in the soluble fraction of total A β (sum of A β 40 and A β 42) was also marginally lower in *clu*^{-/-};5 \times FAD mice at 5 months of age (by 27.3%; P = 0.0994) (Supplementary Figure S2D). However, the ratio of A β aggregates to total A β tended to be higher in *clu*^{-/-};5 \times FAD mice than that in *clu*^{+/+};5 \times FAD mice at each age (Supplementary Figure S2F). Further, when we compared the levels of A β 40 and A β 42, the ratio of total A β 40 to total A β 42 was somewhat higher in *clu*^{-/-};5 \times FAD mice than that in *clu*^{+/+};5 \times FAD mice at each age (by 32.7% or 23.7%; P = 0.1603 or 0.0695) (Supplementary Figure S2G), whereas the ratio of soluble A β 40 to soluble A β 42 was about twice higher in *clu*^{-/-};5 \times FAD mice at 5 months of age (by 91.0%, P = 0.0229), with the lack of *clu* genotype-related difference at 10 months (by 5.1%, P = 0.7502) (Supplementary Figure S2H).

We also measured the loads of 4G8-immunoreactive or Congo red-positive amyloid deposits or plaques (Figure 3A). At 5 months of age, compared with *clu*^{+/+};5 \times FAD mice, *clu*^{-/-};5 \times FAD mice had a lower load of 4G8-immunoreactive amyloid deposits and fewer Congo red-positive amyloid plaques (by 40.4% and 43.1%; P = 0.0154 and 0.0004, respectively), which reflect the deposition of all forms of APP and A β , and the fraction of insoluble A β fibrils, respectively (Figure 3B). Thereafter, the loads substantially increased in the *clu*^{-/-};5 \times FAD mice so that by 10 months of age, there were no *clu* genotype-related differences

(Figure 3B). Finally, the ratios of Congo red-positive amyloid plaques to 4G8-immunoreactive amyloid deposits did not significantly differ between the two *clu* genotypes at 5 or 10 months of age. Instead, the ratios were significantly decreased with age in both *clu* genotypes (P = 0.0015 for *clu*^{-/-};5 \times FAD mice or P = 0.0004 for *clu*^{+/+};5 \times FAD mice) (Supplementary Figure S2I).

Considered together, these quantitative results indicate that clusterin expression is correlated with amyloid deposition at the early age in 5 \times FAD mice, but the effects decline or disappear with age.

Effects of clusterin deficiency on A β -induced neuronal or synaptic loss

The neuropathology of AD includes loss of neurons and synapses as well as A β deposition. Thus, to determine the involvement of clusterin in A β -induced neuronal or synaptic degeneration, we compared the expression of neuronal or synaptic marker proteins using Western blot analysis (Figure 4). The proteins with striking changes in expression included neuronal specific NeuN, nonphosphorylated neurofilament protein SMI-32 (52), presynaptic synaptophysin, axon initial segment-specific and voltage-gated sodium channels-associated ankyrin G (47), post-synaptic PSD-95, vesicle-associated membrane protein (VAMP; synaptobrevin) and postsynaptic scaffold protein ProSAP2/Shank 3 (15). The levels of the neuron- and synapse-specific proteins were significantly lower in 5-month-old *clu*^{+/+};5 \times FAD mice than those in nontransgenic wild-type mice, but were significantly increased in the age-matched *clu*^{-/-};5 \times FAD mice. However, the protein expressions in *clu*^{-/-};5 \times FAD mice were decreased by 10 months of age to the levels as those in *clu*^{+/+};5 \times FAD mice.

Cognitive and motor performance in clusterin-null 5 \times FAD mice

Finally, to determine whether clusterin is involved in cognitive and behavioral impairment during the development of AD, we evaluated the effect of genetic deletion of clusterin on cognitive and motor performance in 5 \times FAD mice.

To evaluate the effects of clusterin on spatial learning and memory performance, the mice were trained in a Morris water maze (MWM) with 3 trials every day for

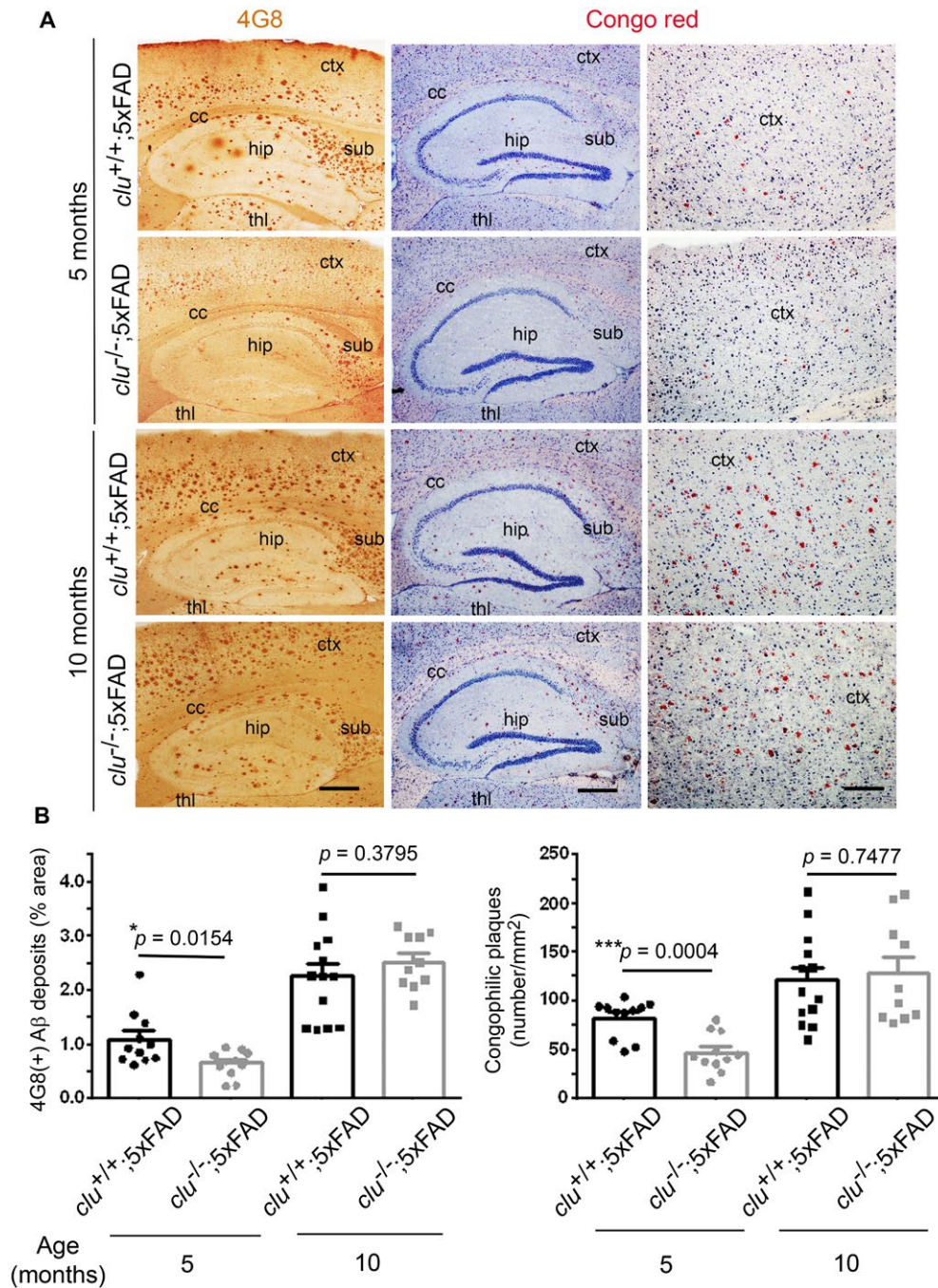


Figure 3. Quantification of amyloid deposits or plaques by immunohistochemical or Congo red staining. **A.** Sagittal brain sections of 5- or 10-month-old *clu*^{+/+};*5xFAD* and *clu*^{-/-};*5xFAD* mice were stained with anti-Aβ(17–24) antibody (4G8) or Congo red dye to detect pan-amyloid precursor protein (APP)/amyloid-β (Aβ)-immunoreactive deposits (1st column, brown dots), or compact amyloid plaques (2nd and 3rd column, red dots). hip, hippocampus; ctx, cortex; thl, thalamus; cc, corpus callosum; sub, subiculum. Scale bars, 500 μm (1st and 2nd column) or 200 μm (3rd column). **B.** The

per cent area of 4G8-immunoreactive amyloid deposits (left graph) or the total number of congophilic amyloid plaques (right graph) in the same brain region of interest was measured in five brain sections per animal, taken every 200 μm lateral from the midline. Numbers (males and females) of animals in each group were 11 (5 and 6; for 5-month-old *clu*^{+/+};*5xFAD*), 11 (5 and 6; for 5-month-old *clu*^{-/-};*5xFAD*), 13 (6 and 7; for 10-month-old *clu*^{+/+};*5xFAD*), or 10 (5 and 5; for 10-month-old *clu*^{-/-};*5xFAD* mice). **P* < 0.05, ***P* < 0.01, or ****P* < 0.001. at wileyonlinelibrary.com]

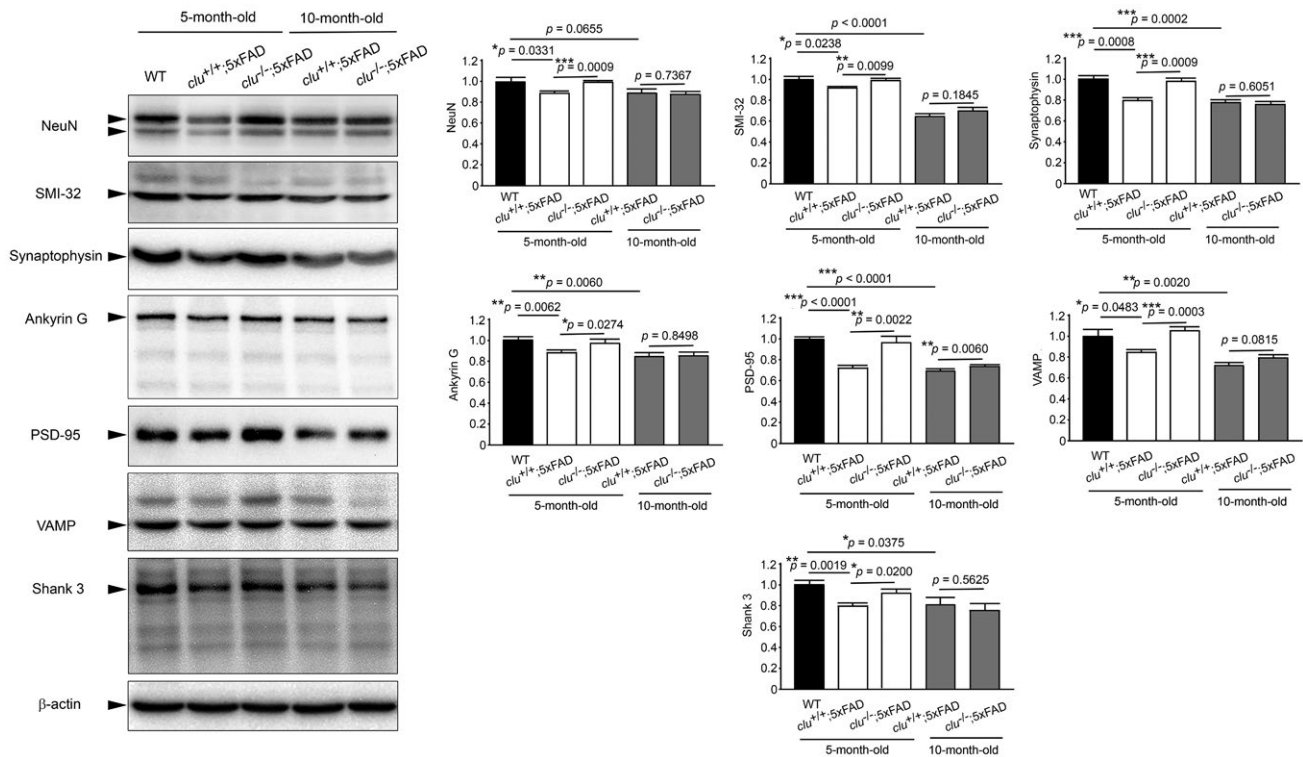


Figure 4. Effect of clusterin and age on expression of neuronal or synaptic proteins in the brain of 5x FAD mouse. **A.** Representative Western blots show expression of neuronal or synaptic proteins in 5- and 10-month-old *clu*^{+/-};5x FAD and *clu*^{-/-};5x FAD mice and 5-month-old nontransgenic wild-type (WT) mice, representing only results with significant differences in expression; neuronal specific NeuN (molecular size, 46–48 kD), nonphosphorylated neurofilament SMI-32 (200 kD), presynaptic synaptophysin (38 kD), axon initial segment-specific and voltage-gated sodium channels-associated ankyrin G (190 kD), postsynaptic PSD-95 (95 kD), vesicle-associated membrane protein

(VAMP, synaptobrevin; 16 kD), postsynaptic scaffold protein ProSAP2/ Shank3 (180 kD) and β -actin (42 kD). **B–H.** Densitometric quantification of indicated proteins after normalization to β -actin. Graphs show significant differences in the levels of the indicated proteins (arrows in blots) between nontransgenic wild-type and 5x FAD mice and between 5-month-old *clu*^{+/-};5x FAD and *clu*^{-/-};5x FAD mice but not between 10-month-old *clu*^{+/-};5x FAD and *clu*^{-/-};5x FAD mice. Protein levels are shown as values relative to a control (black bars, wild-type mice). Bars denote mean \pm SEM of three independent experiments. Each group includes 6 mice (3 males and 3 females). * $P < 0.05$, ** $P < 0.01$, or *** $P < 0.001$.

5 days (Figure 5A). Unexpectedly, both 5-month-old *clu*^{-/-};5x FAD mice and nontransgenic wild-type mice found the platform significantly more quickly than the *clu*^{+/-};5x FAD mice of same age on the first day of training ($P = 0.0021$ and 0.0183 , respectively). Thereafter, the 5-day repeated trainings led to significant improvement in locating the hidden platform for every group of 5-month-old mice, although the nontransgenic wild-type mice and *clu*^{-/-};5x FAD mice were consistently and significantly faster than *clu*^{+/-};5x FAD mice. On the last trial day, *clu*^{-/-};5x FAD mice were able to locate the platform more rapidly than *clu*^{+/-};5x FAD mice ($P = 0.0004$), indicating that clusterin deficiency promoted better spatial learning performance in 5-month-old 5x FAD mice. Three hours later, the animals underwent a free swim probe test to evaluate recall for the previous location of the target platform, a measure of spatial reference memory retention in trained animals (Figure 5B–F). Comparing the speed or the mean distance in reaching the target zone where the escape platform had been located, the number of times the target zone was crossed, and the time spent in the target quadrant,

we found that 5-month-old *clu*^{+/-};5x FAD mice had impaired performance relative to their nontransgenic wild-type littermates. Age-matched *clu*^{-/-};5x FAD mice had significantly better spatial memory performance than the *clu*^{+/-};5x FAD mice. However, this good level of performance did not persist till 10 months of age in the mice with genetic deletion of clusterin. There were no differences between 10-month-old *clu*^{-/-};5x FAD and *clu*^{+/-};5x FAD mice in performance of MWM and probe trials (Figure 5A–F).

After completion of the MWM test, the animals underwent 3 days of training on a balance beam task (Figure 6). On the first trial day, nontransgenic wild-type littermates more rapidly reached the other end, followed by *clu*^{-/-};5x FAD mice, with the *clu*^{+/-};5x FAD mice being the slowest; these differences, however, were not statistically significant. However, by the third day, the 5-month-old wild-type mice and *clu*^{-/-};5x FAD mice moved into the escape chamber increasingly quickly ($P = 0.0363$ and 0.0036 , respectively), spending a significantly shorter time on the beam compared with the age-matched *clu*^{+/-};5x FAD mice ($P = 0.0011$ and 0.0008 , respectively). In contrast, at 10

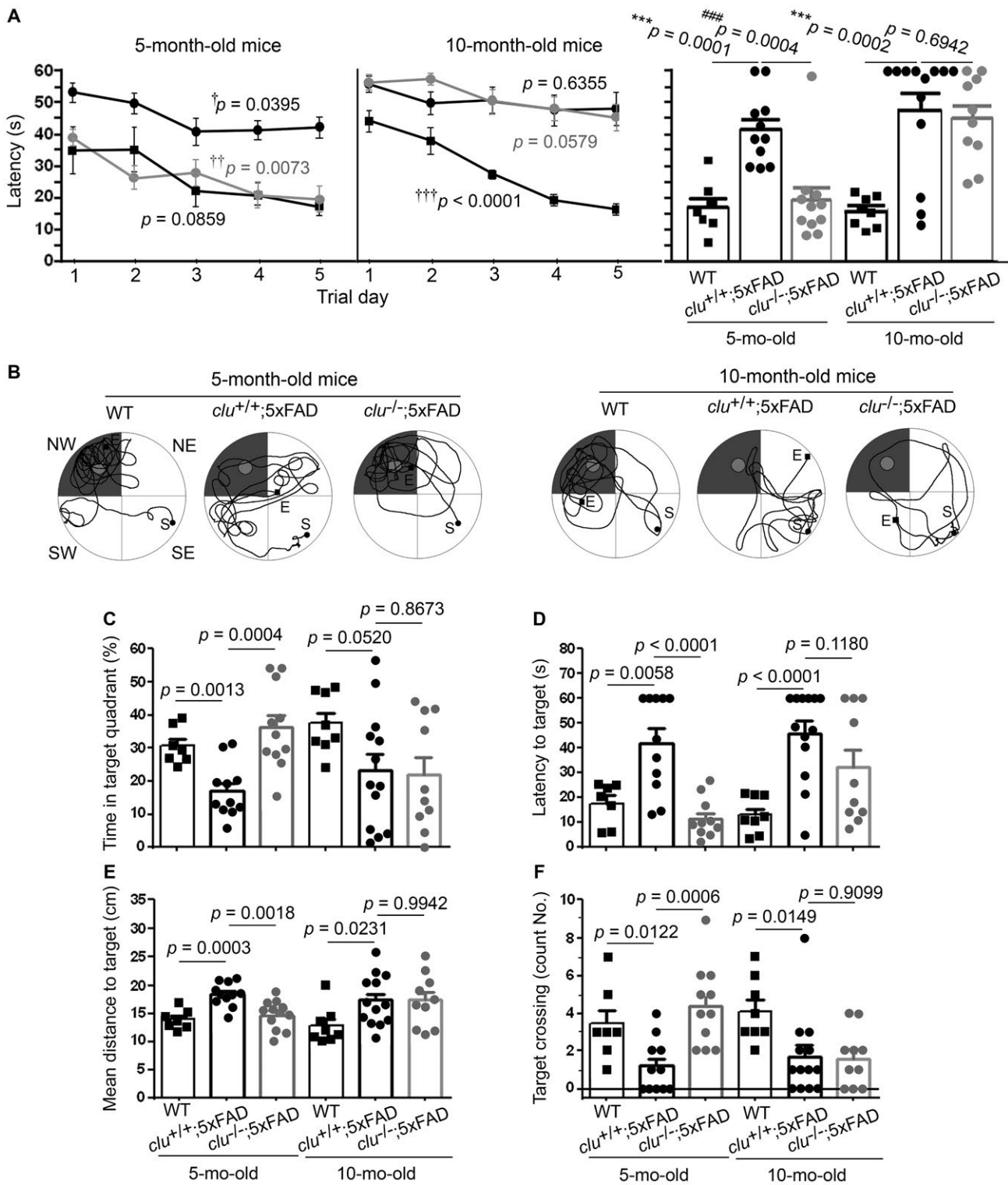


Figure 5. Effect of clusterin on performance of spatial learning and memory in 5×FAD mice. **A.** Animals were trained daily to find a hidden platform in a Morris water maze (MWM). The time taken to find the platform was significantly longer over 5 days in *clu*^{+/+};5×FAD mice (black circles) compared with their nontransgenic wild-type littermates (rectangles). The *clu*^{-/-};5×FAD mice (gray circles) were significantly faster than *clu*^{+/+};5×FAD mice at 5 months of age (left graph), but at 10 months of age, they performed no better than *clu*^{+/+};5×FAD mice (right graph). Crosses (†) denote the effect of 5 days of trainings on the time to reach the target platform in each group (by one-way ANOVA with Student–Newman–Keuls post hoc test). †*P* < 0.05, ††*P* < 0.01, or †††*P* < 0.001. Vertical bars on the right panel denote the values of latency time taken by each animal group on the last trial day. **B–F.** After the training, 60 s-probe trials were performed to evaluate the entire path taken (**B**; from points “S” to “E”) and the percentage of time spent in the target zone (northwest shadow

quadrant in **B**) searching for the platform that had been removed (small circular area in target quadrant in **B**) (**C**) as well as time (**D**) and mean distance (**E**) taken to get the first touch to the target location, and the frequency at which the target location was crossed (**F**). The *clu*^{+/+};5×FAD mice performed poorly on all evaluations compared with nontransgenic wild-type mice. The *clu*^{-/-};5×FAD mice at 5 months of age performed as well as the wild-type littermates at 5 months of age, but at 10 months of age, their performance was as poor as the *clu*^{+/+};5×FAD mice. Numbers (males and females) of animals in each group were 11 (5 and 6; for 5-month-old *clu*^{+/+};5×FAD), 11 (5 and 6; for 5-month-old *clu*^{-/-};5×FAD), 13 (6 and 7; for 10-month-old *clu*^{+/+};5×FAD), or 10 (5 and 5; for 10-month-old *clu*^{-/-};5×FAD mice). Asterisk (*) and pound (#) denote the comparisons between *clu*^{+/+};5×FAD and nontransgenic wild-type mice and between *clu*^{+/+};5×FAD and *clu*^{-/-};5×FAD mice, respectively (by an unpaired *t*-test). **P* < 0.05, ***P* < 0.01, or ****P* < 0.001.

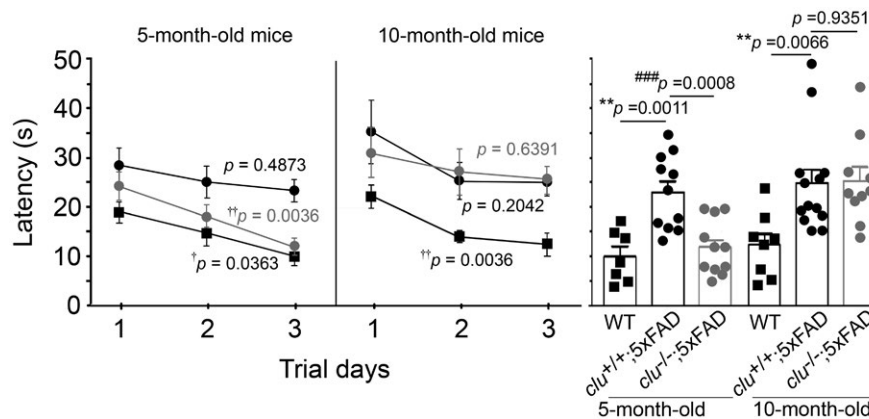


Figure 6. Effect of clusterin on balance and motor coordination in 5×FAD mice. At 5 months of age, *clu*^{-/-};5×FAD mice (gray circles) and wild-type mice (rectangles) reached the escape chamber at the opposite end of the beam significantly faster over 3 days of trials than *clu*^{+/+};5×FAD mice (black circles) (left graph). However, by 10 months of age, the *clu*^{-/-};5×FAD mice took significantly longer than before and were now as slow as *clu*^{+/+};5×FAD mice (right graph), both genotypes of 5×FAD mice being significantly slower than 10-month-old wild-type mice. Vertical bars on the right panel denote the values of latency time taken by each animal group on the last trial day. Numbers (males and

females) of animals in each group were 11 (5 and 6; for 5-month-old *clu*^{+/+};5×FAD), 11 (5 and 6; for 5-month-old *clu*^{-/-};5×FAD), 13 (6 and 7; for 10-month-old *clu*^{+/+};5×FAD), or 10 (5 and 5; for 10-month-old *clu*^{-/-};5×FAD mice). Asterisk (*) and pound (#) signs denote comparisons between *clu*^{+/+};5×FAD and wild-type mice and between *clu*^{+/+};5×FAD and *clu*^{-/-};5×FAD mice, respectively (by an unpaired *t*-test). **P* < 0.05, ***P* < 0.01, or ****P* < 0.001. Crosses (†) denote the effect of 3 days of training on the time to reach the escape chamber in each group (by one-way ANOVA with Student–Newman–Keuls post hoc test). †*P* < 0.05 or ††*P* < 0.01.

months of age, *clu*^{-/-};5×FAD and *clu*^{+/+};5×FAD mice both failed to acquire the capability to run along the beam with the balance and motor coordination achieved by nontransgenic wild-type mice (*P* = 0.6391, 0.2042 and 0.0036, respectively). Thus, there were no differences between the two *clu* genotypes of 5×FAD mice on the third day of balance beam task (*P* = 0.9351) (Figure 6).

DISCUSSION

Since clusterin can maintain Aβ solubility by preventing Aβ aggregation (32) and promote its clearance from brain by mediating BBB transport (3,57), early interest in clusterin was centered on defining its protective role against AD. Experimental support for this possibility came from

findings that clusterin alleviated Aβ toxicity in neuronal cells (4,29,56). However, growing evidence suggests that clusterin interacts with Aβ to enhance its neurotoxicity and cause neurodegeneration (23,25,40,41). A previous study with hAPP transgenic PDAPP mice (10) provided the first evidence of an *in vivo* functional role for clusterin, with its absence leading to fewer amyloid plaques and lesser neuritic dystrophy despite a consistent level in total Aβ. Similarly with our present study of 5×FAD mice, a recent study (55) also found a marked decrease in total amyloid deposition containing soluble and insoluble Aβ as well as parenchymal amyloid plaques in clusterin-null APP/PS1 mice. Although the different findings concerning the deposition of total Aβ likely came from the different background features of hAPP transgenic mice used (55), it is important

that clusterin deficiency prevented amyloid deposition and A β -induced neurodegeneration in the hAPP transgenic mouse models of AD.

In the present study, we observed interactions between clusterin and A β proteins in the brains of 5 \times FAD mice. Both mRNA and protein levels of clusterin were higher in 5 \times FAD mice than in age-matched wild-type littermates, a finding similar to that in the brains of human patients with AD compared with controls without dementia (14,33,40). While clusterin levels did not significantly change with age in wild-type mice, they substantially increased with age in 5 \times FAD mice. In addition, the expression of DKK-1, a Wnt antagonist mediating clusterin-driven A β toxicity (23,45), was also significantly higher and increased with age in 5 \times FAD mice. These findings indicate that A β deposition causes increased expressions of clusterin and DKK-1 in the hAPP-transgenic mouse models (46). Next, we detected colocalization of A β and clusterin in nearly all compact amyloid plaques in 5 \times FAD mice, which is similar to that found in the brains of AD patients (8,22,34). Furthermore, we found that A β and clusterin were in the same complex as they were co-immunoprecipitated with each other in brain lysates of 5 \times FAD mice. Because clusterin was detected together with A β proteins of various sizes in our co-IP experiment, it is thought that clusterin has the propensity to bind or interact with different forms of A β , such as monomers, oligomers, or fibril aggregates *in vivo*. Using purified or synthetic proteins, many studies have shown that clusterin binds to A β proteins with high affinity (2,13,31,37).

This study provides the first *in vivo* evidence that clusterin-directed A β deposition and oligomerization augment A β neurotoxicity and underlie AD pathogenesis in hAPP transgenic mice. Although knockdown of clusterin was previously shown to reduce A β toxicity in primary neurons (23), we further elucidated how genetic loss of clusterin influences AD pathology in 5 \times FAD mice. Clusterin deficiency led to less A β (total, soluble and insoluble A β 40 and A β 42) and fewer amyloid plaques in the brains of 5 \times FAD mice at 5 months of age. Clusterin binding could render A β resistant to proteolytic degradation and maintain its stability (32,37); therefore, *clu*^{+/+};5 \times FAD mice would exhibit higher amyloid deposition than *clu*^{-/-};5 \times FAD mice. Alternatively, the reduced level of A β likely is due to the decrease in A β generation in *clu*^{-/-};5 \times FAD mice.

However, we specifically paid attention to A β oligomers and A β aggregates because A β neurotoxicity is primarily attributed to its oligomer forms rather than its monomer or fibril forms (25,40,41). A β 42 is considered to be more neurotoxic than A β 40 because of its propensity to more readily aggregate into oligomers (16,30,48,53). Clusterin, then, could sequester or stabilize toxic A β oligomers so that they are less degradable, or inhibit further aggregation of A β oligomers into nontoxic fibrils (32,37). When compared the results of ELISA quantification in *clu*^{-/-};5 \times FAD mice with those in *clu*^{+/+};5 \times FAD mice, level of soluble A β 42, in which include A β 42 oligomers, was more reduced than that of soluble A β 40 or insoluble A β 42, with the most dramatic reduction in soluble A β oligomers. The

difference in A β aggregates composed of A β oligomers, protofibrils and fibrils, was not statistically significant. Next, we found no *clu* genotype-related difference in the ratio of soluble A β /total A β or insoluble A β /total A β , whereas the ratio of soluble A β oligomers/total A β , soluble A β oligomers/total soluble A β , or soluble A β oligomers/A β aggregates was markedly lower in *clu*^{-/-};5 \times FAD mice. The ratio of A β aggregates/total A β became rather somewhat higher. We further found that lack of clusterin caused lower loads of 4G8-immunoreactive plaques and fewer Congo red-positive fibrillar amyloid plaques, which are representative of total A β deposition and insoluble A β aggregates, respectively. The ratios of Congo red-positive plaques/4G8-immunoreactive plaques were similar in both *clu* genotypes of 5 \times FAD mice. Finally, 5-month-old *clu*^{-/-};5 \times FAD mice had less neuronal and synaptic loss as evaluated by the expression of neuronal or synaptic proteins. These mice also had significantly better motor and cognitive performances. Collectively, these results suggest that clusterin is involved in amyloid pathogenesis responsible for neurodegeneration and behavioral impairment seen in the 5 \times FAD mouse model of early AD, perhaps by facilitating A β production and deposition or by shifting A β composition toward more toxic soluble A β oligomers.

However, it should be noted that any influence of clusterin deficiency on AD pathology declined or disappeared with age. By 10 months of age, all A β pools in *clu*^{-/-};5 \times FAD mice had significantly increased to levels similar to those in *clu*^{+/+};5 \times FAD mice. There were no detectable differences in amyloid plaque deposition, neuronal and synaptic loss, or motor and cognitive impairment between the two *clu* genotypes of 5 \times FAD mice. These findings reminded us of the previous human brain studies that demonstrated an association of clusterin with AD pathology in early stage. In longitudinal cohort analyses combining volumetric MRI scans with quantification of clusterin and A β proteins, plasma clusterin levels were associated with atrophy in brain regions affected in AD (21,50). More importantly, an interaction between A β 42 and clusterin has been exclusively related with atrophy of the entorhinal cortex, a region that is selectively affected early in the pathogenesis of AD (5,51). In cognitively normal older individuals and those with mild cognitive impairment (MCI), decreased levels of CSF A β 42 (related to increased brain A β 42 deposition) and elevated CSF clusterin levels were associated with higher entorhinal cortex volume loss but not with hippocampal atrophy (11). The A β -clusterin association with entorhinal cortical atrophy was stronger in those individuals than in patients with advanced AD. Together with these human cohort studies, our findings that clusterin deficiency was associated with a significantly lower degree of amyloid pathology, neuronal and synaptic loss and behavioral and cognitive impairment in 5-month-old mice but not in 10-month-old mice suggest that clusterin may facilitate amyloid pathogenesis and induce A β -directed neurodegeneration in the early stages of AD (11,28,50).

Currently, it is unclear how clusterin can have disparate effects on the early and late stages of AD pathogenesis.

One possible explanation is that the effect of clusterin on A β neurotoxicity may depend upon a substoichiometric ratio of clusterin and A β (54). Earlier *in vitro* studies showed that clusterin modulates amyloid pathogenesis in a biphasic manner to promote or inhibit its neurotoxicity. A higher proportion of clusterin in an A β -clusterin complex could cause relatively less A β aggregation and toxicity, whereas a lower proportion could facilitate A β aggregation and increase toxicity (4,19,41,56). Our present study supports that hypothesis because we observed that, with age, levels of A β increased to a greater extent than those of clusterin. In the brains of 10-month-old 5 \times FAD mice, total A β (sum of A β 40 and A β 42) and A β 42 were elevated by 39.6% and 37.4%, respectively, relative to values in 5-month-old 5 \times FAD mice. While clusterin levels also increased from 5 to 10 months of age, the 17.3% increase was relatively smaller than that of A β proteins. The resulting decline in the ratio of clusterin to A β may affect amyloid pathogenesis, thereby aggravating neurodegeneration and behavioral or cognitive impairment (36). A further possibility is that as AD progresses into the later stages with a rapid increase in A β deposition, the clusterin content might become insufficient to mediate amyloid pathogenesis and other more amyloidogenic factors such as phosphorylated tau (p-tau) or Apo E may become more prominent. Corroborating this hypothesis, we noticed that, by 10 months of age, *clu*^{-/-};5 \times FAD mice had levels of amyloid pathology, neuronal and synaptic loss and motor and cognitive impairment comparable to those of *clu*^{+/+};5 \times FAD mice. A prior study in Apo E and clusterin double knockout PDAPP mice (9) showed that the concurrent absence of Apo E and clusterin caused earlier onset and larger amyloid deposition, suggesting that clusterin can modify the structure, accumulation, deposition and toxicity of A β in cooperation with Apo E. In addition, a human brain study (11) found that interaction only between clusterin and A β was associated with volume loss in the entorhinal cortex in cognitively normal elderly people, whereas in those with MCI, atrophy was also related to the interaction of p-tau and A β . Moreover, they showed that interaction between A β and p-tau was significantly associated with later atrophy in the hippocampus or other temporal lobe regions, which was not the case with the interaction of clusterin and A β . Therefore, these findings support the contention that other factors such as Apo E or p-tau have a stronger influence than clusterin on AD pathology in the later stages.

A recent study is of note because it investigated the effect of clusterin deficiency on amyloid pathology in APP/PS1 transgenic mice (55), describing the role of clusterin in A β transport across the BBB via low-density lipoprotein receptor-related protein-2 (LRP2) (3). They found a marked decrease in amyloid deposition in the brain parenchyma but a parallel increase in cerebral amyloid angiopathy (CAA) in *clu*^{-/-};APP/PS1 mice. As CAA is likely due to amyloid deposition on the cerebral vessel walls along the perivascular drainage pathways (1), it could be indicative of an abnormal A β clearance in AD brain. Mounting evidence suggests that A β 40 has a stronger propensity to promote CAA relative to A β 42, and thus the higher A β 40/

A β 42 ratio favors toward CAA development (12,18). When we briefly compared the levels of A β 40 and A β 42 in our 5 \times FAD mice, the A β 40/A β 42 ratio was significantly increased in the soluble fractions of 5 months-old *clu*^{-/-};5 \times FAD mice, supporting the previous findings (49,55). However, there was a statistically nonsignificant increase in the ratio of total A β 40/A β 42, and the ratio differences disappeared at 10 months. While these differences in A β 40/A β 42 ratio might represent the effect of clusterin deficiency on CAA in 5 \times FAD mice, it would be warranted to explore the expression of CAA in clusterin-wildtype or -null 5 \times FAD mice in order to define the roles of clusterin in A β clearance or transport *in vivo*.

In conclusion, clusterin preferentially augments the toxic A β pools to facilitate the early stage of AD pathogenesis, and thereby promotes A β -directed neurodegeneration and behavioral and cognitive impairments. However, as the pathology progresses, its influences decline, suggesting that substances other than clusterin may be more critical in the later stages. Therefore, a strategy to reduce the level of clusterin or to inhibit clusterin-A β interactions may provide potential therapeutic opportunities for AD in early stage, but it should be considered whether such a treatment can consistently retard the disease pathogenesis in later advanced stages.

ACKNOWLEDGMENTS

This work was supported by the National Research Foundation of Korea (NRF-2015R1A2A1A15052049 and NRF-2017R1D1A1B03030567) and by the Asan Institute for Life Sciences, Asan Medical Center, Seoul, Korea (2016-396).

DECLARATIONS

The authors declare no conflict of interest.

REFERENCES

- Alonzo NC, Hyman BT, Rebeck GW, Greenberg SM (1998) Progression of cerebral amyloid angiopathy: Accumulation of amyloid-beta 40 in affected vessels. *J Neuropathol Exp Neurol* **57**:353–359.
- Beeg M, Stravalaci M, Romeo M, Carra AD, Cagnotto A, Rossi A *et al* (2016) Clusterin binds to Abeta1-42 oligomers with high affinity and interferes with peptide aggregation by inhibiting primary and secondary nucleation. *J Biol Chem* **291**:6958–6966.
- Bell RD, Sagare AP, Friedman AE, Bedi GS, Holtzman DM, Deane R, Zlokovic BV (2007) Transport pathways for clearance of human Alzheimer's amyloid beta-peptide and apolipoproteins E and J in the mouse central nervous system. *J Cereb Blood Flow Metab* **27**:909–918.
- Boggs LN, Fuson KS, Baez M, Churgay L, McClure D, Becker G, May PC (1996) Clusterin (Apo J) protects against *in vitro* amyloid-beta (1-40) neurotoxicity. *J Neurochem* **67**:1324–1327.
- Braak H, Braak E (1991) Neuropathological staging of Alzheimer-related changes. *Acta Neuropathol* **82**:239–259.

6. Calero M, Rostagno A, Matsubara E, Zlokovic B, Frangione B, Ghiso J (2000) Apolipoprotein J (clusterin) and Alzheimer's disease. *Microsc Res Tech* **50**:305–315.
7. Cascella R, Conti S, Tatini F, Evangelisti E, Scartabelli T, Casamenti F *et al* (2013) Extracellular chaperones prevent Abeta42-induced toxicity in rat brains. *Biochim Biophys Acta* **1832**:1217–1226.
8. Choi-Miura NH, Ihara Y, Fukuchi K, Takeda M, Nakano Y, Tobe T, Tomita M (1992) SP-40,40 is a constituent of Alzheimer's amyloid. *Acta Neuropathol* **83**:260–264.
9. DeMattos RB, Cirrito JR, Parsadanian M, May PC, O'Dell MA, Taylor JW *et al* (2004) ApoE and clusterin cooperatively suppress A beta levels and deposition: Evidence that ApoE regulates extracellular A beta metabolism *in vivo*. *Neuron* **41**:193–202.
10. DeMattos RB, O'Dell MA, Parsadanian M, Taylor JW, Harmony JA, Bales KR *et al* (2002) Clusterin promotes amyloid plaque formation and is critical for neuritic toxicity in a mouse model of Alzheimer's disease. *Proc Natl Acad Sci U S A* **99**:10843–10848.
11. Desikan RS, Thompson WK, Holland D, Hess CP, Brewer JB, Zetterberg H *et al* (2014) The role of clusterin in amyloid-beta-associated neurodegeneration. *JAMA Neurol* **71**:180–187.
12. Fryer JD, Simmons K, Parsadanian M, Bales KR, Paul SM, Sullivan PM, Holtzman DM (2005) Human apolipoprotein E4 alters the amyloid-beta 40:42 ratio and promotes the formation of cerebral amyloid angiopathy in an amyloid precursor protein transgenic model. *J Neurosci* **25**:2803–2810.
13. Ghiso J, Matsubara E, Koudinov A, Choi-Miura NH, Tomita M, Wisniewski T, Frangione B (1993) The cerebrospinal-fluid soluble form of Alzheimer's amyloid beta is complexed to SP-40,40 (apolipoprotein J), an inhibitor of the complement membrane-attack complex. *Biochem J* **293**(Pt 1):27–30.
14. Giannakopoulos P, Kovari E, French LE, Viard I, Hof PR, Bouras C (1998) Possible neuroprotective role of clusterin in Alzheimer's disease: A quantitative immunocytochemical study. *Acta Neuropathol* **95**:387–394.
15. Grabrucker AM, Schmeisser MJ, Udvardi PT, Arons M, Schoen M, Woodling NS *et al* (2011) Amyloid beta protein-induced zinc sequestration leads to synaptic loss via dysregulation of the ProSAP2/Shank3 scaffold. *Mol Neurodegener* **6**:65.
16. Hardy JA, Higgins GA (1992) Alzheimer's disease: The amyloid cascade hypothesis. *Science* **256**:184–185.
17. Harold D, Abraham R, Hollingworth P, Sims R, Gerrish A, Hamshere ML *et al* (2009) Genome-wide association study identifies variants at CLU and PICALM associated with Alzheimer's disease. *Nat Genet* **41**:1088–1093.
18. Herzig MC, Winkler DT, Burgermeister P, Pfeifer M, Kohler E, Schmidt SD *et al* (2004) A beta is targeted to the vasculature in a mouse model of hereditary cerebral hemorrhage with amyloidosis. *Nat Neurosci* **7**:954–960.
19. Hughes SR, Khorkova O, Goyal S, Knaeblein J, Heroux J, Riedel NG, Sahasrabudhe S (1998) Alpha2-macroglobulin associates with beta-amyloid peptide and prevents fibril formation. *Proc Natl Acad Sci U S A* **95**:3275–3280.
20. Humphreys DT, Carver JA, Easterbrook-Smith SB, Wilson MR (1999) Clusterin has chaperone-like activity similar to that of small heat shock proteins. *J Biol Chem* **274**:6875–6881.
21. Hye A, Riddoch-Contreras J, Baird AL, Ashton NJ, Bazenet C, Leung R *et al* (2014) Plasma proteins predict conversion to dementia from prodromal disease. *Alzheimers Dement* **10**:799–807 e2.
22. Kida E, Choi-Miura NH, Wisniewski KE (1995) Deposition of apolipoproteins E and J in senile plaques is topographically determined in both Alzheimer's disease and Down's syndrome brain. *Brain Res* **685**:211–216.
23. Killick R, Ribe EM, Al-Shawi R, Malik B, Hooper C, Fernandes C *et al* (2014) Clusterin regulates beta-amyloid toxicity via Dickkopf-1-driven induction of the wnt-PCP-JNK pathway. *Mol Psychiatry* **19**:88–98.
24. Lambert JC, Heath S, Even G, Campion D, Sleegers K, Hiltunen M *et al* (2009) Genome-wide association study identifies variants at CLU and CR1 associated with Alzheimer's disease. *Nat Genet* **41**:1094–1099.
25. Lambert MP, Barlow AK, Chromy BA, Edwards C, Freed R, Liosatos M *et al* (1998) Diffusible, nonfibrillar ligands derived from Abeta1-42 are potent central nervous system neurotoxins. *Proc Natl Acad Sci U S A* **95**:6448–6453.
26. Lee JY, Cho E, Seo JW, Hwang JJ, Koh JY (2012) Alteration of the cerebral zinc pool in a mouse model of Alzheimer disease. *J Neuropathol Exp Neurol* **71**:211–222.
27. Livak KJ, Schmittgen TD (2001) Analysis of relative gene expression data using real-time quantitative PCR and the 2(-Delta Delta C(T)) method. *Methods* **25**:402–408.
28. Malkki H (2014) Alzheimer disease: Chaperone protein clusterin is involved in amyloid-beta-associated entorhinal atrophy in early AD. *Nat Rev Neurol* **10**:60.
29. Mannini B, Cascella R, Zampagni M, Van Waarde-Verhagen M, Meehan S, Roodveldt C *et al* (2012) Molecular mechanisms used by chaperones to reduce the toxicity of aberrant protein oligomers. *Proc Natl Acad Sci U S A* **109**:12479–12484.
30. Masters CL, Simms G, Weinman NA, Multhaup G, McDonald BL, Beyreuther K (1985) Amyloid plaque core protein in Alzheimer disease and down syndrome. *Proc Natl Acad Sci U S A* **82**:4245–4249.
31. Matsubara E, Frangione B, Ghiso J (1995) Characterization of apolipoprotein J-Alzheimer's a beta interaction. *J Biol Chem* **270**:7563–7567.
32. Matsubara E, Soto C, Governale S, Frangione B, Ghiso J (1996) Apolipoprotein J and Alzheimer's amyloid beta solubility. *Biochem J* **316**(Pt 2):671–679.
33. May PC, Lampert-Etchells M, Johnson SA, Poirier J, Masters JN, Finch CE (1990) Dynamics of gene expression for a hippocampal glycoprotein elevated in Alzheimer's disease and in response to experimental lesions in rat. *Neuron* **5**:831–839.
34. McGeer PL, Kawamata T, Walker DG (1992) Distribution of clusterin in Alzheimer brain tissue. *Brain Res* **579**:337–341.
35. McLaughlin L, Zhu G, Mistry M, Ley-Ebert C, Stuart WD, Florio CJ *et al* (2000) Apolipoprotein J/clusterin limits the severity of murine autoimmune myocarditis. *J Clin Invest* **106**:1105–1113.
36. Miners JS, Clarke P, Love S (2017) Clusterin levels are increased in Alzheimer's disease and influence the regional distribution of Abeta. *Brain Pathol* **27**:305–313.
37. Narayan P, Meehan S, Carver JA, Wilson MR, Dobson CM, Klenerman D (2012) Amyloid-beta oligomers are sequestered by both intracellular and extracellular chaperones. *Biochemistry* **51**:9270–9276.

38. Narayan P, Orte A, Clarke RW, Bolognesi B, Hook S, Ganzinger KA *et al* (2011) The extracellular chaperone clusterin sequesters oligomeric forms of the amyloid-beta(1-40) peptide. *Nat Struct Mol Biol* **19**:79–83.
39. Oakley H, Cole SL, Logan S, Maus E, Shao P, Craft J *et al* (2006) Intraneuronal beta-amyloid aggregates, neurodegeneration, and neuron loss in transgenic mice with five familial Alzheimer's disease mutations: Potential factors in amyloid plaque formation. *J Neurosci* **26**:10129–10140.
40. Oda T, Pasinetti GM, Osterburg HH, Anderson C, Johnson SA, Finch CE (1994) Purification and characterization of brain clusterin. *Biochem Biophys Res Commun* **204**:1131–1136.
41. Oda T, Wals P, Osterburg HH, Johnson SA, Pasinetti GM, Morgan TE *et al* (1995) Clusterin (apoJ) alters the aggregation of amyloid beta-peptide (A beta 1-42) and forms slowly sedimenting a beta complexes that cause oxidative stress. *Exp Neurol* **136**:22–31.
42. Poon S, Easterbrook-Smith SB, Rybchyn MS, Carver JA, Wilson MR (2000) Clusterin is an ATP-independent chaperone with very broad substrate specificity that stabilizes stressed proteins in a folding-competent state. *Biochemistry* **39**:15953–15960.
43. Poon S, Rybchyn MS, Easterbrook-Smith SB, Carver JA, Pankhurst GJ, Wilson MR (2002) Mildly acidic pH activates the extracellular molecular chaperone clusterin. *J Biol Chem* **277**:39532–39540.
44. Poon S, Treweek TM, Wilson MR, Easterbrook-Smith SB, Carver JA (2002) Clusterin is an extracellular chaperone that specifically interacts with slowly aggregating proteins on their off-folding pathway. *FEBS Lett* **513**:259–266.
45. Purro SA, Dickins EM, Salinas PC (2012) The secreted Wnt antagonist Dickkopf-1 is required for amyloid beta-mediated synaptic loss. *J Neurosci* **32**:3492–3498.
46. Rosi MC, Luccarini I, Grossi C, Fiorentini A, Spillantini MG, Prisco A *et al* (2010) Increased Dickkopf-1 expression in transgenic mouse models of neurodegenerative disease. *J Neurochem* **112**:1539–1551.
47. Santuccione AC, Merlini M, Shetty A, Tackenberg C, Bali J, Ferretti MT *et al* (2013) Active vaccination with ankyrin G reduces beta-amyloid pathology in APP transgenic mice. *Mol Psychiatry* **18**:358–368.
48. Snyder SW, Ladror US, Wade WS, Wang GT, Barrett LW, Matayoshi ED *et al* (1994) Amyloid-beta aggregation: Selective inhibition of aggregation in mixtures of amyloid with different chain lengths. *Biophys J* **67**:1216–1228.
49. Suzuki N, Iwatsubo T, Odaka A, Ishibashi Y, Kitada C, Ihara Y (1994) High tissue content of soluble beta-1-40 is linked to cerebral amyloid angiopathy. *Am J Pathol* **145**:452–460.
50. Thambisetty M, An Y, Kinsey A, Koka D, Saleem M, Guntert A *et al* (2012) Plasma clusterin concentration is associated with longitudinal brain atrophy in mild cognitive impairment. *Neuroimage* **59**:212–217.
51. Thambisetty M, Simmons A, Velayudhan L, Hye A, Campbell J, Zhang Y *et al* (2010) Association of plasma clusterin concentration with severity, pathology, and progression in Alzheimer disease. *Arch Gen Psychiatry* **67**:739–748.
52. Thangavel R, Sahu SK, Van Hoesen GW, Zaheer A (2009) Loss of nonphosphorylated neurofilament immunoreactivity in temporal cortical areas in Alzheimer's disease. *Neuroscience* **160**:427–433.
53. Walsh DM, Klyubin I, Fadeeva JV, Cullen WK, Anwyl R, Wolfe MS *et al* (2002) Naturally secreted oligomers of amyloid beta protein potently inhibit hippocampal long-term potentiation *in vivo*. *Nature* **416**:535–539.
54. Wilson MR, Yerbury JJ, Poon S (2008) Potential roles of abundant extracellular chaperones in the control of amyloid formation and toxicity. *Mol Biosyst* **4**:42–52.
55. Wojtas AM, Kang SS, Olley BM, Gatherer M, Shinohara M, Lozano PA *et al* (2017) Loss of clusterin shifts amyloid deposition to the cerebrovasculature via disruption of perivascular drainage pathways. *Proc Natl Acad Sci U S A* **114**:E6962–E6971.
56. Yerbury JJ, Poon S, Meehan S, Thompson B, Kumita JR, Dobson CM, Wilson MR (2007) The extracellular chaperone clusterin influences amyloid formation and toxicity by interacting with prefibrillar structures. *FASEB J* **21**:2312–2322.
57. Zlokovic BV, Martel CL, Mackic JB, Matsubara E, Wisniewski T, McComb JG *et al* (1994) Brain uptake of circulating apolipoproteins J and E complexed to Alzheimer's amyloid beta. *Biochem Biophys Res Commun* **205**:1431–1437.

SUPPORTING INFORMATION

Additional supporting information may be found in the online version of this article at the publisher's web site:

Figure S1. Expressions of mRNA and protein of DKK-1 in the brains of 5-month-old wild-type (WT), and 5- or 10-month-old 5×FAD mice.

Figure S2. Relative proportions of various pools of AB proteins in the brains of *clu*^{+/+};5×FAD and *clu*^{-/-};5×FAD mice.